2018 7th IEEE International Conference on Biomedical
Robotics and Biomechatronics (Biorob)
Enschede, The Netherlands, August 26-29, 2018

# Resistance is Not Futile: Haptic Damping Forces Mitigate Effects of Motor Noise During Reaching

Arvid Q.L. Keemink, Niek Beckers and Herman van der Kooij

*Abstract*— **Understanding how users adapt their motor behavior to damping forces can improve assistive haptic shared control strategies, for instance in heavy robot-assisted lifting applications. In previous experiments we showed that subjects reaching in constant and position-dependent longitudinal damping fields were able to reduce their movement time and increase end-point accuracy. The movement time versus movement distance and prescribed end-point accuracy agreed with Fitts' Law. However, why subjects were able to have shorter movement time while subjected to impeding damping forces is not explained by Fitts' Law. Based on the minimal variance principle we propose that humans exploit the noise-filtering behavior of constant or position-dependent damping forces. These damping forces attenuate mechanical effects of activation-dependent motor noise. This allows for higher motor activation and shorter movement time without losing end-point accuracy. Consequently, higher allowed motor activation allows for higher accelerations that lead to higher peak velocities, resulting in shorter movement times. Linear and non-linear stochastic optimal feedback control and optimal estimation models with multiplicative noise corroborate measurement data, supporting our hypothesis.**

## I. Introduction

A human's mechanical power and force capabilities can be augmented by assistive devices. Such devices amplify or complement the user's force or display forces to steer and inform the user. Virtual fixtures, such as potential force fields, have been used as haptic force sources to assist humans in tasks in haptic tele-operation or during power augmentation [1]. If there is any relevant intelligence in the modulation of location and impedance of these virtual fixtures, the haptic method can be regarded as haptic shared control [2]. Shared control uses haptic forces and change in device impedance to give cues, increase safety, assist movements or force the user to change movement strategy. In previous work [3] we proposed a simple shared controller based on controlled variable damping forces around reaching targets, i.e. position dependent damping or PDD. Such a force can be used to support a person's movements during human-machine cooperative tasks of picking and placing of heavy objects, while being completely passive.

Haptic viscous damping is a force that mimics a physical dissipative force. This force ($F$) is proportional through a damping coefficient ($b$) to the velocity of movement ($v$) in the form $F = -bv$ where $b > 0$. In contrast to potential forces, like stiffness, damping forces are more 'forgiving' by allowing users to move against them, albeit at the cost of expending more energy. Furthermore, damping forces are passive in the sense that they can only dissipate energy from a mechanical system, making dissipative assistive devices inherently stable and safe during interaction with human users.

Constantly moving a device in a viscous damping field will unnecessarily increase a user's energy expenditure. Therefore, damping can be made position-dependent by making the damping coefficient change and increase near important task-related movement targets. Viscous damping can be low initially, such that the user can move unimpeded, and ramp up when closing in to a task-relevant location, assisting the user to reach the location accurately and assisting with deceleration.

If the device consistently applies these damping forces around task-relevant locations on the user, (s)he will change his/her reaching movement plans accordingly. Motor adaptation research has mainly focused on orthogonal force perturbations during longitudinal arm reaching movements (e.g. orthogonal force fields [4] or Coriolis forces [5]), but not on how humans adapt their movement strategy to *longitudinal* damping forces opposing the movement. Although these orthogonal (curl) forces and longitudinal (damping) forces are both velocity dependent, the former is an active force (see similar reasoning of anti-symmetric stiffness in [6]) that steers the human reaching movement off-course, while the latter is a passive force that impedes the movement. Therefore, any conclusions drawn about curl-field adaptation cannot be directly applied to longitudinal damping.

A number of studies investigated the effect of damping-like forces on the performance and kinematics of human motor tasks. Previous research showed that reaching underwater increased reaching movement times (MT) [7], [8]. The underwater environment is viscously dissipative, as well as highly inertial. Other authors showed that constant static friction helped in reducing reaching times and increasing accuracy for moving *low* masses during reaching [9–11]. Crommentuijn et al. [11] found that increasing the Coulomb friction magnitude did not negatively impact reaching accuracy but only decreased the likability of the task. The authors hypothesized that friction forces provide a predictable constant deceleration and act as a filter to unintentional movement. However, they did not investigate the influence of friction or damping forces when subjects move high masses. Furthermore, they did not focus on how movement and force

This research was supported by the Dutch Technology Foundation (TTW), which is part of the Dutch Organisation for Scientific Research (NWO), and which is partly funded by the Ministry of Economic Affairs. Project Number: 12162.

All authors are with the group of Biomechanical Engineering, Faculty of Engineering Technology, University of Twente, 7500 AE Enschede, The Netherlands a.q.l.keemink@utwente.nl.

978-1-5386-8183-1/18/$31.00 ©2018 IEEE

profiles changed after adaptation to the friction forces and how to explain or predict the steady-state change in human movement strategies.

Our previous research [3] showed that constant damping and PDD *both* increased steady-state reaching performance in terms of reduced MT and increased end-point accuracy, for moving a mass of 12.5 kg. This mass was chosen to be much heavier than the average human arm to resemble the movement of a large weight. The relation between MT and demanded accuracy (specified by index of difficulty) followed Fitts' Law for all damping conditions. Because of its accuracy, simplicity and utility, Fitts' Law is a widely used model for predicting movement time for fast, aimed, arm movements, with a good fit to empirical data [12]. However, it gives no insight into *why* constant damping and PDD resulted in better reaching performance compared to reaching without damping.

Literature shows that humans adapt and generalize their reaching strategies based on their own limb dynamics, state-dependent environment dynamics or artificial haptic forces [4], [5], [13–16]. Evidence suggests that humans use two different internal models during coordinated reaching: a forward model (efferent copy of control through forward dynamics), using an internal representation of the body and environment to predict the body state [17], and an inverse model [18] to calculate the motor commands needed to perform a movement in a combined feed-forward and feedback controlled fashion. Although this explains how control is carried out, it does not explain how humans adapt to different environment dynamics.

It has been proposed that humans perform their movements in some optimal way. Bell-shaped velocity profiles and apparent trajectory smoothness seen in reaching movements are due to some optimality principle. Harris and Wolpert [19] proposed that the central nervous system (CNS) optimizes reaching by minimizing the deviation at the target position; called the minimum variance model. This model is based on the fact that the neural signals and force production in the human body are subjected to noise. They stated that the motor command signals are characterized by *signal-dependent noise* or *multiplicative motor noise*. This means that higher muscle activation results in higher levels of muscle force noise. Their first-order estimation was that the standard deviation of this noise increases *linearly* with the mean force output [20].

This movement uncertainty due to noise has to be optimally integrated in a movement plan to make an optimal movement. For each new environment, in our experiment the damping condition, the motor plan is reoptimized for those dynamics [21]. Therefore, a proposed model is the one of stochastic optimal control and optimal estimation [22], [23], that captures the signal-dependent noise together with metabolic energy expenditure in a stochastic optimal control framework.

In this model, the CNS predicts sensory consequences of our motor commands using the forward model. These predictions are combined with delayed sensory information from proprioception and vision to infer the state of the body and environment (optimal state estimation) [24]. The optimal state estimate is used using the inverse model to optimally tune the feedback-control gains to maximize some measure of performance (optimal control) [25].

Several mathematical stochastic optimal control and optimal estimation methods, known as Linear Quadratic Gaussian (LQG) methods, have been put forth to mathematically model reaching movements, showing high agreement with empirical data [16], [23–25].

In this work, we asked ourselves why damping forces allow for faster movement times, and how users adapted their movement plan when subjected to these damping forces. Furthermore we attempt to explain steady-state performance results through a computational model. Our computational analysis indicates that deterministic, or consistent and predictable, damping attenuates mechanical effects of multiplicative motor noise allowing for faster arm movements while retaining target acquisition accuracy. Understanding how users adapt their motor behavior to damping forces can improve assistive haptic shared control strategies, for instance in robot-assisted heavy lifting applications.

Building on the minimal variance principle and stochastic optimal control models, our hypothesis is that damping forces assist in reducing end-point variance introduced by both additive and multiplicative motor noise. Subjects have to guarantee an end-point variance sufficient to perform and successfully finish the task. This requested end-point variance is *not* necessarily minimal, but sufficient for the requested target size. Therefore, subjects can apply high control forces that would lead to more end-point variance in the absence of (position dependent) damping. This, in result, leads to shorter movement times. Evidence that corroborates this hypothesis will be discussed in the following sections by using models of stochastic optimal control and optimal estimation.

## II. Dynamics and Optimal Control of the Reaching Task

In the experiment described in [3] we compared three movement conditions (C1, C2 and C3) where 18 subjects performed reaching tasks with a 1D haptic manipulandum simulating a mass of 12.5 kg while feeling different longitudinal damping forces. These three conditions were also compared to a damping-free baseline condition (B). The damping force was proportional to the velocity of movement by the damping coefficient as shown in Fig. 1. Subjects were instructed to reach the target as quickly as possible over a distance between 18 and 28 cm within target sizes ranging from 0.41 cm to 2.71 cm diameter.

The reaching dynamics of this task are modeled after Todorov [23], Diedrichsen [26] and Izawa and Shadmehr [24]. We believe it is sufficient to neglect multi-link arm dynamics and simplify the dynamics to a single degree of freedom point mass on which a damper acts. The human force is generated by the neural input signal $u(t)$ that passes through two first-order low-pass filters, both with time

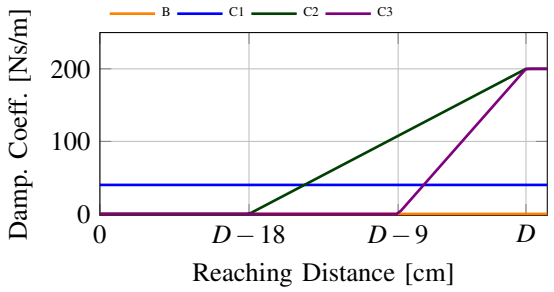


Fig. 1: Damping coefficients for each condition. Conditions B1 and B2 have zero damping coefficient. Condition C1 has a constant coefficient of 40 Ns/m. In conditions C2 and C3 the coefficient increases linearly in value from 0 Ns/m to 200 Ns/m when approaching the target at movement distance $D$.

constant $\tau$, to model the activation dynamics and calcium dynamics of the muscle.

The continuous-time dynamics of this problem has five states $\mathbf{x}(t) = [x(t), \dot{x}(t), f(t), h(t), g(t)]^T$, where $x(t)$ is the position of moved mass $m$, $\dot{x}(t)$ is the mass velocity, $f(t)$ is the force the human applies onto the mass, $h(t)$ is the intermediate state of the low-pass filtered neural activation, and $g(t)$ is the target location of the reaching movement that is chosen a priori.

### A. Dynamical Model

The *noise-free* equations of motion of the aforementioned dynamics are given by

$$m\ddot{x}(t) = -b(x)\dot{x}(t) + f(t)$$
$$\dot{f}(t) = \frac{h(t) - f(t)}{\tau}, \; \dot{h}(t) = \frac{u(t) - h(t)}{\tau},$$

where $\ddot{x}(t)$ is the mass acceleration and $b(x)$ is the position dependent damping coefficient.

The discrete-time (time instant $k$, time step $\delta$) state evolution equations are given by

$$\begin{bmatrix} x_{k+1} \\ \dot{x}_{k+1} \\ f_{k+1} \\ h_{k+1} \\ g_{k+1} \end{bmatrix} = \begin{bmatrix} 1 & \delta & 0 & 0 & 0 \\ 0 & 1 - \frac{\delta b(x)}{m} & \frac{\delta}{m} & 0 & 0 \\ 0 & 0 & 1 - \frac{\delta}{\tau} & \frac{\delta}{\tau} & 0 \\ 0 & 0 & 0 & 1 - \frac{\delta}{\tau} & 0 \\ 0 & 0 & 0 & 0 & 1 \end{bmatrix} \begin{bmatrix} x_k \\ \dot{x}_k \\ f_k \\ h_k \\ g_k \end{bmatrix} + \begin{bmatrix} 0 \\ 0 \\ 0 \\ \frac{\delta}{\tau} \\ 0 \end{bmatrix} u_k$$
$$\mathbf{x}_{k+1} = \mathbf{A}(x)\mathbf{x}_k + \mathbf{B}u_k.$$

The damping coefficient $b(x)$ is given by

$$b(x) = \begin{cases} 0, & \text{if no damping,} \\ b_c, & \text{if constant damping,} \\ b_s \max\{0, x(t) - x_0\}, & \text{if PDD,} \end{cases} \quad (1)$$

with constant parameters: damping coefficient $b_c$, damping coefficient slope $b_s$ and positional offset $x_0$. The PDD is zero for $x(t) \leq x_0$ and ramps up with slope $b_s$ for $x(t) > x_0$.

The system dynamics are influenced by zero-mean Gaussian white noise ($\mathcal{N}(\mathbf{0}, \Omega)$) with specified covariance $\Omega = \sigma\sigma^T$ where $\sigma$ is a vector of standard deviations. The relevant noise sources are:

- noise with unit variance that will be scaled by neural activation $\xi_k \sim \mathcal{N}(0, 1)$,
- process noise $\omega_k \sim \mathcal{N}(\mathbf{0}, \sigma_\omega \sigma_\omega^T)$,
- measurement noise $\nu_k \sim \mathcal{N}(\mathbf{0}, \sigma_\nu \sigma_\nu^T)$ that acts on position, velocity and force state.

With process noise and uncertain observation the total model dynamics become

$$\mathbf{x}_{k+1} = \mathbf{A}(x)\mathbf{x}_k + (\mathbf{B} + \Gamma\xi_k)u_k + \omega_k \quad (2)$$
$$\mathbf{y}_k = \mathbf{C}\mathbf{x}_k + \nu_k.$$

Matrix $\mathbf{C}$ picks the states to be observed by the CNS. Vector $\Gamma = [0\ 0\ 0\ \sigma_u\ 0]^T$ scales the unit noise variance of $\xi_k$ and positions it in the proper state equation for $h(t)$ (as outlined in [21] and [23]). All noise amplitudes are scaled by $\sqrt{\delta}$ to normalize the random walk process [27], [28].

### B. Optimal Control of the Reaching Task

An optimal controller and estimator can be designed for the dynamics described in (2), lasting for time instants $k = 1, \ldots, N$. The modeled task is a reaching movement where the hand starts at an initial position and moves to a target position $g_k$ in a *pre-specified* time interval $M$ and dwells inside the target until terminal time $N$. This period of duration $N - M$ is the *dwell period*.

The optimal controller minimizes the expected quadratic cost

$$J = \mathbb{E}\left\{ \mathbf{x}_N^T \mathbf{Q}_N \mathbf{x}_N + \sum_{k=1}^{N-1} \left( \mathbf{x}_k^T \mathbf{Q}_k \mathbf{x}_k + R_k u_k^2 \right) \right\}, \quad (3)$$

with $\mathbb{E}\{\cdot\}$ the expected value of a stochastic variable. Parameter $R_k > 0$ denotes the relative cost on energy expenditure, which penalizes high control signals, and therefore influences the level of multiplicative motor noise. The state dependent cost can be given as $\mathbf{Q}_k \succeq 0$ during the reaching movement, or as terminal cost $\mathbf{Q}_N \succeq 0$. The terminal cost is held constant during the whole dwell period. To enforce the reaching movement towards target $g_k$ the cost matrix $\mathbf{Q}$ is comprised of

$$\mathbf{Q}_k = \mathbf{0}_{5\times 5}, \text{ for } k = 1, \ldots, M-1,$$
$$\mathbf{Q}_k = \begin{bmatrix} w_p & 0 & 0 & 0 & -w_p \\ 0 & w_v & 0 & 0 & 0 \\ 0 & 0 & w_f & 0 & 0 \\ 0 & 0 & 0 & 0 & 0 \\ -w_p & 0 & 0 & 0 & w_p \end{bmatrix}, \text{ for } k = M, \ldots, N,$$

where time indices $k = 1, \ldots, M-1$ denote the movement time, and indices $k = M, \ldots, N$ denote the dwell period where the subject had to keep the cursor in the target. Cost weights $w_p$, $w_v$ and $w_v$ relatively weight the contributions of positioning error, velocity and used force respectively.

The optimal controller that minimizes (3) is a Linear Quadratic Gaussian (LQG) controller capable of handling multiplicative motor noise in the control input. Please refer to [21] and [23] for an elaborate derivation of such a controller.

## III. Model Simulation and Comparison with Experimental Data

In this section we compare some of the results of the experiment with the simulated model results. The model had fixed weight values of: $w_p = 10^7$, $w_v = 10^5$, $w_p = 10^2$ and $R_k = 1$. The mass was $m = 12.5$ kg, the filter time constant $\tau = 40$ ms [23] and the time step $\delta = 10$ ms.

The models were simulated with three damping $b(x)$ conditions. The first condition consists of a constant damping of $b_c = 40$ Ns/m (labeled C1). Conditions C2 and C3 consisted of two different position-dependent damping (PDD), see (1). Slope offset distance was $x_0 = 0.09$ m for C2 and $x_0 = 0.18$ m for C3. The slope of the damping coefficient was $b_s = 20/9$ kNs/m$^2$ for C2 and $b_s = 10/9$ kNs/m$^2$ for C3. As a reference, we also simulated the dynamical model without damping, denoted as baseline (B).

The required optimal controller is different for constant damping conditions (i.e. linear dynamics with no damping or constant damping) and position dependent damping conditions (i.e. non-linear and state-dependent PDD). For linear and non-linear dynamics we use two different types of LQG methods:

1) LTI LQG: This model solves for the optimal controller for a linear time-invariant (LTI) system with additive measurement noise, additive process noise and activation-dependent (i.e. multiplicative with the control signal) noise [21], [23]. A Kalman filter estimates the states of the system that are disturbed by measurement noise. We use this model to investigate the difference in behavior, such as endpoint variance, between additive and multiplicative noise, without non-linear behavior influencing the results.
2) iLQG: In the case of non-linear dynamics, when $b(x)$ is *not* constant and state-dependent (i.e. PDD), the optimal controller is an iterative LQG (iLQG) controller [27], [28]. This model solves for the approximately optimal controller for the dynamical system with non-linear dynamics introduced by a position dependent damping value. This model is chosen to explain salient features of the movement and force profiles and to show how damping reduces the endpoint variance of performed reaching movements.

### A. Movement and Force Profiles

Fig. 2 shows the movement profiles of three subjects performing reaching movements (over a distance of $D = 0.18$ m and target $ID = 3.5$ bits for all four relevant conditions [3]). Salient features of the measured movement profiles include

- B and C1: the symmetrical bell-shaped velocity profiles. The force profiles are symmetrical in magnitude for B, but asymmetrical for C1, since the damper helps with slowing down.
- C2: the velocity profile is slightly asymmetrical with a longer stretched tail in the deceleration phase. The relative moment in time of peak velocity is earlier, compared to B and C1. Furthermore, there is no need for the subjects to apply a deceleration force.
- C3: the velocity profile is asymmetrical, with a ‘sharp

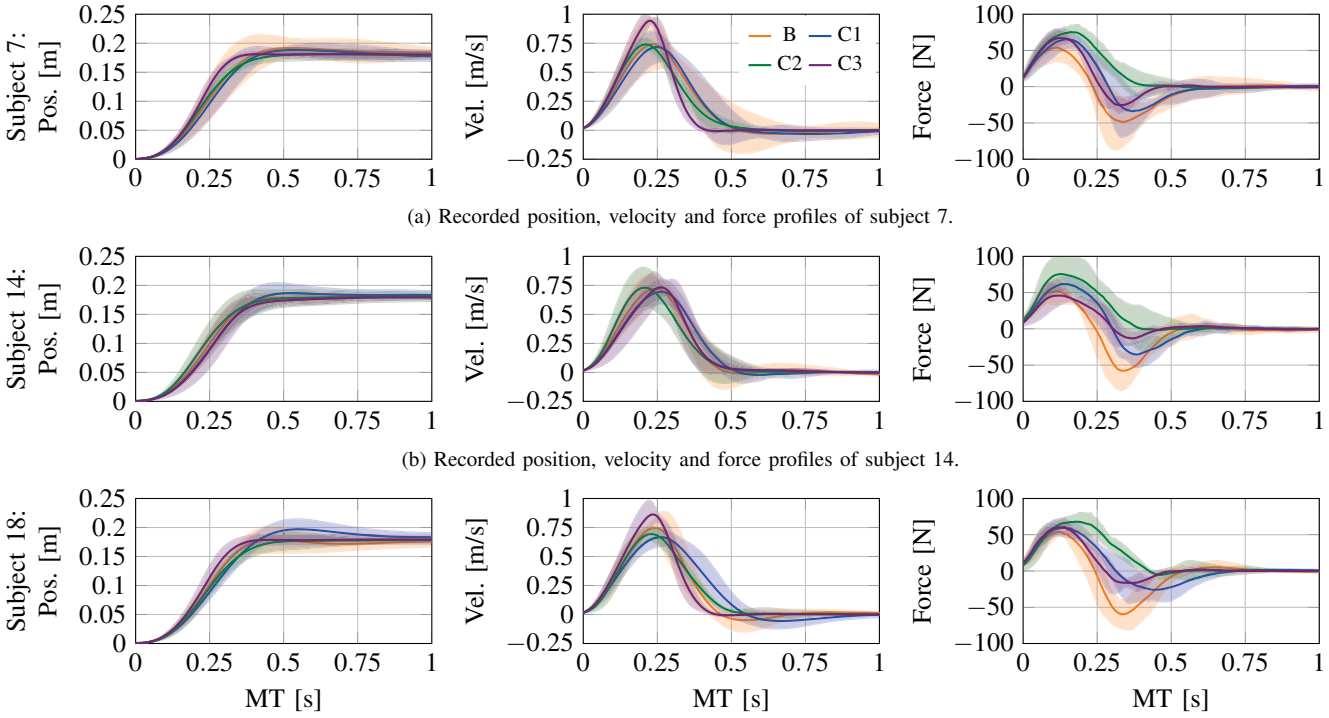


(a) Recorded position, velocity and force profiles of subject 7.

(b) Recorded position, velocity and force profiles of subject 14.

(c) Recorded position, velocity and force profiles of subject 18.

Fig. 2: Recorded movement and force profiles of subjects 7, 14 and 18, reproduced from [3]. The solid curves show the mean of the movements after learning. The shaded area shows ±1 standard deviation. The legend in the top-center subfigure applies to all subfigures.

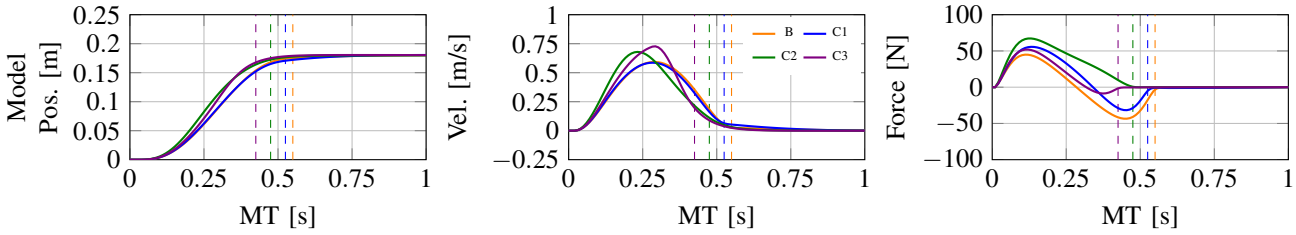


(a) (b) (c)

Fig. 3: Simulated mean movement profiles for the three damping condition and baseline. a) Position profiles, b) velocity profiles, and c) force profiles produced by the iLQG method and the non-linear dynamical model. Dwell time starts at: 0.55 s for B, 0.525 s for C1, 0.475 s for C2 and at 0.425 s for C3, indicated with a colored dashed line. Notice the same asymmetry in the velocity profiles for C2 (longer right tail) and C3 (sharp drop-off on the right) as is visible in the experimental data in Fig. 2. The legend in b) applies to all subfigures.

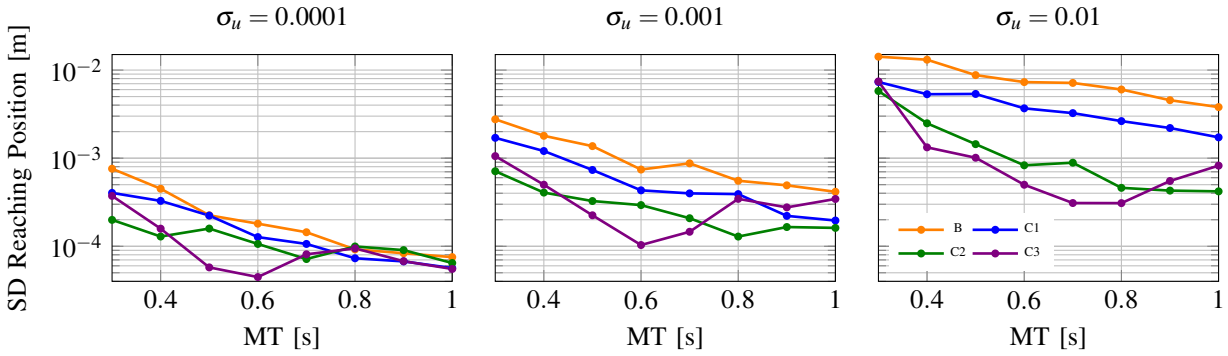


(a) (b) (c)

Fig. 4: Numerical results of the end-point standard deviation versus movement time. a–c) Different multiplicative noise scaling factors $\sigma_u$: the standard deviation in reached end-point position taken from 40 movement repetitions of the iLQG method and the non-linear dynamical model at the end of the dwell period, for different MT. The legend in c) applies to all subfigures.

bend' near the peak velocity with fast deceleration. The relative moment in time of peak velocity is later, close to the onset of the damping. The force profiles are asymmetrical in magnitude since the damper helps in slowing down.

Fig. 3 shows the simulated mean movement profiles for the linear and non-linear models. The salient features visible in the experimental data can be seen in the simulation results: the asymmetry in force profile magnitude and the asymmetry in velocity bell-shapes for C2 and C3. Asymmetry in the force value might be thought of as the optimal controller exploiting useful effects and complementing opposing effects of the damper force. Velocity and force profile asymmetry in timing (i.e. skewing) is a result of an optimization process. These results hints at the fact that reaching movements subjected to time-varying damping can be well explained and predicted by optimization methods such as optimal control. It shows that humans re-optimize their movement plan for the different dynamical conditions [24].

### B. Influence of Noise Variance

*1) Multiplicative Noise and Fitts' Law:* The non-linear dynamical model was run with activation-dependent noise with three different noise standard deviation scaling values $\sigma_u = 0.0001$, 0.001 and 0.01 in (2). The movement time was varied from 0.3 to 1.0 s with added dwell time of 0.5 s. The model was run 40 times to get a measure of end-point accuracy calculated by the standard deviation in reaching position.

The numerical results of these models for the three $\sigma_u$ values, three damping conditions and baseline are shown in Fig. 4. For all simulations, end-point position standard deviation decreases (i.e. accuracy increases) with increasing movement time. Also, all damping conditions increase the model's end-point accuracy compared to the baseline. This might explain the reduced MT for conditions C1, C2 and C3 observed in the experiment. To achieve similar reaching accuracy for e.g. C1 as in B, we notice that this movement can be performed with less MT. This relative trend between conditions is true for all values of $\sigma_u$.

Notable is the minimum in variance for the C3 condition for an MT around 0.6–0.8 s, after which it increases. We cannot say with certainty whether minimal variance would actually be achieved in real reaching tasks for those specific MTs. Possibly, demanding a slow movement ($> 0.8$ s) through an increasing damping field (i.e. C3) might require more neural activation for a longer time, which in turn actually reduces end-point accuracy.

*2) Additive Noise versus Multiplicative Noise:* To investigate the relative effect of multiplicative and additive noise on end-point variability, the LQG model was run for conditions B and C1 with either a) multiplicative motor noise ($\sigma_u = 0.3$), or b) a combination of additive observation noise and process noise ($\sigma_\omega = 5$ N, $\sigma_v = [0.025\text{ m}, 0.1\text{ m/s}, 6.5\text{ N}, 0, 0]^T$). The parameter values were chosen to show similar movement variance visually, as the observed variance during movements

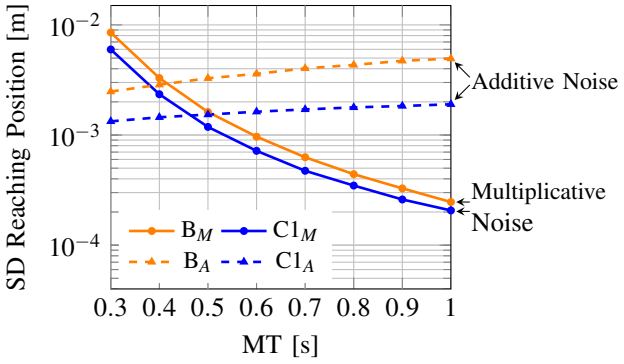


Fig. 5: Contributions additive process noise and signal-dependent noise on end-point accuracy. End-point accuracy for experimental conditions B (no-damping baseline) and C1 (constant damping). The additive process and measurement noise (subscript '*A*' for additive, dashed lines) in the LQG model shows that for larger MT the end-point variance increases. This is different from neural activation dependent noise (subscript '*M*' for multiplicative, solid line). Damping forces filter contributions of all noise sources. The model results were averaged over 10,000 movement repetitions.

used to produce Fig. 4. The MT of the reaching movement was varied from 0.3 to 1.0 s with added dwell time of 0.5 s. The model was run 10,000 times to calculate the end-point accuracy.

The end-point variance increases with MT for additive noise, as is shown in Fig. 5. This trend is in contrast to the trend for dynamics with multiplicative motor noise alone. It would imply that taking a longer MT would result in less accurate movements. This is neither in accordance with Fitts' Law, nor with observation. Therefore, a model with large additive noise cannot be a model that describes the variance of our reaching dynamics. Nevertheless, some amount of additive noise is unavoidable in the human's motor system. Adding damping forces reduces end-point variance for both the multiplicative noise (this is a reconfirmation of the results for B and C1 in Fig. 4) as well as for additive noise.

## IV. Discussion and Future Work

The aim of this work was to give qualitative evidence that dissipative damping reduces end-point variance by allowing more motor activation and subsequently reducing movement time during reaching tasks [3]. This knowledge is useful for developing controllers that modulate damping forces generated by devices during physical human-robot interaction and cooperation. The shown model results might allow for the design of the optimal position dependent 'shape' of the damping coefficient. In that case the optimality criterion might be dependent on both preferred MT and subjective preference, i.e. smoothness and maximum effort, of the user.

Through a model-based analysis and comparison to empirical data [3], we investigated how additive and signal-dependent motor noise influence reaching behavior, end-point variance and movement time. The model simulations show that end-point accuracy increases with increasing movement time, according to Fitts' Law. Analyzing the effects of additive and signal-dependent noise showed that signal-dependent motor noise can explain the increase in reaching accuracy, whereas additive noise does not.

Performing optimally controlled movements with the same cost function and same MT shows reaching kinematics with smaller end-point variance in conditions C1, C2 and C3. This corroborates results we presented in [3]. Salient features of movement and force profiles of the models are highly similar to experimental data. This suggests that the models used, and therefore also their response to noise, are an indicator of why subjects managed to reduce their reaching time. Damping force gives subjects the possibility to increase their neural activation and move faster, because it allows them to guarantee a certain targeting variance.

The experimental results, and model results agree with the hypothesis in [11] that the use of friction or damping, in general, shows a noise filtering behavior. Our used models give insight into how this filtering effect happens. The results and model agree with our hypothesis that MT can be reduced because subjects exploit the variance-reducing effect of the damping force, because the task instruction was to reach the target as quickly as possible.

Another way to think about the benefit of constant damping, or PDD, is that it acts as an antagonist muscle whose activation is noise-free and does not contribute to increasing the end-point variance. If this virtual antagonist muscle is 'tuned properly' to activate during a required deceleration or targeting phase, it benefits the subject.

Somewhat in line with the previous statement, the decrease in MT for the damping conditions could be ascribed to implicit role distribution of the subject with the damping field. We suggest the possibility that the subject considered the damping field as another 'agent' which aided the subject in the reaching movement by assisting in the deceleration phase of the movement. Reed et al. [29] showed that two human partners working together on a target acquisition task performed the task faster than individuals performing the same task alone. Through the recorded interaction forces, they observed specialization, in which one partner accelerated and the other partner decelerated the movement. The specialization was hypothesized to be the cause of the faster reaching movement [29].

To investigate this hypothesis in future experiments, artificial multiplicative force noise could be added to the damping force, i.e. noise that scales with the velocity of movement. According to our hypothesis, this should in turn increase MT. If this does not happen it might be more indicative of benefits of human-human role distribution. Although this does not explain *why* this role distribution, with two agents that are both influenced by their own multiplicative motor noise, would result in a shorter MT.

The used optimal control reaching models have their limitations. For physical reaching movements, the MT is an outcome metric of the performed actions. However, in the model, the MT is a predefined parameter. A similar issue is raised in [30] where they ascribe slower movements of Parkinson's disease patients to higher cost on energy. The high cost on energy would henceforth increase MT. However, a model with fixed MT does not show this behavior with different cost on energy expenditure.

This problem can be overcome by adding a non-zero state-dependent cost during the reaching movement *before* the dwell period. However, this would put more cost on being far away from the target, and less cost on being close. This is different from the more reasonable idea of only inducing cost when not ending up at the target. Also, state dependent cost during reaching results in asymmetrical velocity and force profiles that are not observed in free-air human reaching. However, cost during a dwell period or at terminal time does resemble human reaching kinematics very well.

The results of both the experiment and the model are also limited in that they cannot be extrapolated to arbitrary movement masses and arbitrary damping force magnitude. A more realistic muscle model with force saturation would be an extension to identify how humans would re-optimize their reaching strategy for interacting with such heavy mechanical mass or high damping force that they require peak voluntary muscle contraction.

The currently performed experiment was set up mainly to determine how subjects' MT would change for all the damping conditions compared to a no damping condition. The used protocol was not ideal to extract the information to explain the applied strategies with optimal control. There was no comparable measure of end-point accuracy to compare to the model results.

A Fitts' like reaching experiment that demands subjects to dwell in the target introduces more variance in MT than in tapping tasks [3]. A dwell time measurement also eliminates a proper measure of end-point variance. In future research, a more typical two-way tapping task or button-press task, but with high mass, might serve two useful purposes: 1) giving a proper measure of end-point variance and 2) give a better fit to Fitts' law.

Future research might focus more on single distance reaching with e.g. only two target sizes to remove any variance due to target distance and target size. All non-baseline conditions could have constant damping, with smaller steps in value between conditions. This might give more insight in how subjects re-optimize their movement, and (with a better cost on state, or terminal state) how it can be explained with a relative reweighting between targeting error and energy expenditure.

## REFERENCES


[1] L. B. Rosenberg, "The Use of Virtual Fixtures as Perceptual Overlays to Enhance Operator Performance in Remote Environments," DTIC Document, Tech. Rep., 1992.

[2] D. A. Abbink and M. Mulder, "Neuromuscular analysis as a guideline in designing shared control," in *Advances in haptics*. InTech, 2010.

[3] A. Keemink, R. Fierkens, J. Lobo-Prat, J. Schorsch, D. Abbink, J. Smeets, and A. Stienen, "Using position dependent damping forces around reaching targets for transporting heavy objects: A Fitts' law approach," in *Biomedical Robotics and Biomechatronics (BioRob), 2016 6th IEEE International Conference on*. IEEE, 2016, pp. 1323–1329.

[4] R. Shadmehr and F. A. Mussa-Ivaldi, "Adaptive representation of dynamics during learning of a motor task," *Journal of Neuroscience*, vol. 14, no. 5, pp. 3208–3224, 1994.

[5] P. DiZio and J. R. Lackner, "Congenitally blind individuals rapidly adapt to Coriolis force perturbations of their reaching movements," *Journal of Neurophysiology*, vol. 84, no. 4, pp. 2175–2180, 2000.

[6] N. Hogan, "Controlling impedance at the man/machine interface," in *Robotics and Automation, 1989. Proceedings., 1989 IEEE International Conference on*. IEEE, 1989, pp. 1626–1631.

[7] R. Kerr, "Movement time in an underwater environment," *Journal of Motor Behavior*, vol. 5, no. 3, pp. 175–178, 1973.

[8] ——, "Diving, adaptation, and Fitts law," *Journal of Motor Behavior*, vol. 10, no. 4, pp. 255–260, 1978.

[9] C. Richard and M. Cutkosky, "The effects of real and computer generated friction on human performance in a targeting task," in *Proceedings of the ASME Dynamic Systems and Control Division*, vol. 69, 2000, p. 2.

[10] P. Berkelman and J. Ma, "Effects of friction parameters on completion times for sustained planar positioning tasks with a haptic interface," in *Intelligent Robots and Systems, 2006 IEEE/RSJ International Conference on*. IEEE, 2006, pp. 1115–1120.

[11] K. Crommentuijn and D. J. Hermes, "The effect of coulomb friction in a haptic interface on positioning performance," in *Haptics: Generating and Perceiving Tangible Sensations*. Springer, 2010, pp. 398–405.

[12] Y. Guiard and M. Beaudouin-Lafon, "Fitts' law 50 years later: applications and contributions from human–computer interaction," 2004.

[13] S. J. Goodbody and D. M. Wolpert, "Temporal and amplitude generalization in motor learning," *Journal of Neurophysiology*, vol. 79, no. 4, pp. 1825–1838, 1998.

[14] M. A. Conditt and F. A. Mussa-Ivaldi, "Central representation of time during motor learning," *Proceedings of the National Academy of Sciences*, vol. 96, no. 20, pp. 11 625–11 630, 1999.

[15] A. Karniel and F. A. Mussa-Ivaldi, "Sequence, time, or state representation: how does the motor control system adapt to variable environments?" *Biological cybernetics*, vol. 89, no. 1, pp. 10–21, 2003.

[16] R. Shadmehr and S. P. Wise, *The computational neurobiology of reaching and pointing: a foundation for motor learning*. MIT press, 2005.

[17] R. C. Miall and D. M. Wolpert, "Forward models for physiological motor control," *Neural networks*, vol. 9, no. 8, pp. 1265–1279, 1996.

[18] M. Kawato, "Internal models for motor control and trajectory planning," *Current opinion in neurobiology*, vol. 9, no. 6, pp. 718–727, 1999.

[19] C. M. Harris and D. M. Wolpert, "Signal-dependent noise determines motor planning," *Nature*, vol. 394, no. 6695, pp. 780–784, 1998.

[20] K. E. Jones, A. F. d. C. Hamilton, and D. M. Wolpert, "Sources of signal-dependent noise during isometric force production," *Journal of neurophysiology*, vol. 88, no. 3, pp. 1533–1544, 2002.

[21] J. Izawa, T. Rane, O. Donchin, and R. Shadmehr, "Motor adaptation as a process of reoptimization," *Journal of Neuroscience*, vol. 28, no. 11, pp. 2883–2891, 2008.

[22] E. Todorov and M. I. Jordan, "Optimal feedback control as a theory of motor coordination," *Nature neuroscience*, vol. 5, no. 11, pp. 1226–1235, 2002.

[23] E. Todorov, "Stochastic optimal control and estimation methods adapted to the noise characteristics of the sensorimotor system," *Neural computation*, vol. 17, no. 5, pp. 1084–1108, 2005.

[24] J. Izawa and R. Shadmehr, "On-line processing of uncertain information in visuomotor control," *Journal of Neuroscience*, vol. 28, no. 44, pp. 11 360–11 368, 2008.

[25] R. Shadmehr and J. W. Krakauer, "A computational neuroanatomy for motor control," *Experimental Brain Research*, vol. 185, no. 3, pp. 359–381, 2008.

[26] J. Diedrichsen, "Optimal task-dependent changes of bimanual feedback control and adaptation," *Current Biology*, vol. 17, no. 19, pp. 1675–1679, 2007.

[27] E. Todorov and W. Li, "A generalized iterative LQG method for locally-optimal feedback control of constrained nonlinear stochastic systems," in *American Control Conference, 2005. Proceedings of the 2005*. IEEE, 2005, pp. 300–306.

[28] W. Li and E. Todorov, "Iterative linearization methods for approximately optimal control and estimation of non-linear stochastic system," *International Journal of Control*, vol. 80, no. 9, pp. 1439–1453, 2007.

[29] K. Reed and M. Peshkin, "Physical Collaboration of Human-Human and Human-Robot teams," *IEEE Transactions on Haptics*, vol. 1, no. 2, pp. 108–120, 2008.

[30] P. Mazzoni, A. Hristova, and J. W. Krakauer, "Why don't we move faster? Parkinson's disease, movement vigor, and implicit motivation," *Journal of neuroscience*, vol. 27, no. 27, pp. 7105–7116, 2007.